Journal of Medicinal Chemistry

Article

Pyridone-Conjugated Monobactam Antibiotics with Gram-Negative Activity

Matthew F. Brown, Mark J. Mitton-Fry, Joel T Arcari, Rose Barham, Jeffrey Casavant, Brian S Gerstenberger, Seungil Han, Joel R Hardink, Thomas M Harris, Thuy Hoang, Michael D Huband, Manjinder S. Lall, M Megan Lemmon, Chao Li, Jian Lin, Sandra P McCurdy, Eric McElroy, Craig McPherson, Eric S. Marr, John P. Mueller, Lisa Mulllins, Antonia A. Nikitenko, Mark C Noe, Joseph Penzien, Mark S Plummer, Brandon P. Schuff, Veerabahu Shanmugasundaram, Jeremy T. Starr, Jianmin Sun, Andrew P. Tomaras, Jennifer A. Young, and Richard P. Zaniewski

J. Med. Chem., **Just Accepted Manuscript** • DOI: 10.1021/jm400560z • Publication Date (Web): 11 Jun 2013

Journal of Medicinal Chemistry is published by the American Chemical Society. 1155 Sixteenth Street N.W., Washington, DC 20036

Pyridone-Conjugated Monobactam Antibiotics with Gram-Negative Activity

Matthew F. Brown,*[a] Mark J. Mitton-Fry,[a] Joel T. Arcari,[a] Rose Barham,[a] Jeffrey Casavant,[a] Brian S. Gerstenberger,[a] Seungil Han,[e] Joel R. Hardink,[d] Thomas M. Harris,[a] Thuy Hoang,[a] Michael D. Huband,[c] Manjinder S. Lall,[a] M. Megan Lemmon,[c] Chao Li,[a] Jian Lin,[d] Sandra P. McCurdy,[c] Eric McElroy,[a] Craig McPherson,[c] Eric S. Marr,[e] John P. Mueller,[c] Lisa Mullins,[c] Antonia A. Nikitenko,[a] Mark C. Noe,[a] Joseph Penzien,[c] Mark S. Plummer,[a] Brandon P. Schuff,[a] Veerabahu Shanmugasundaram,[b] Jeremy T. Starr,[a] Jianmin Sun,[a] Andrew Tomaras,[c] Jennifer A. Young,[a] Richard P. Zaniewski[c]

[a]Worldwide Medicinal Chemistry, [b]Computational Chemistry, [c]Antibacterials Research Unit, [d]Pharmacokinetics, Dynamics & Metabolism, [e]Structural Biology, Pfizer Global Research and Development, Eastern Point Road, Groton, CT 06340.

ABSTRACT

Herein we describe the structure-aided design and synthesis of a series of pyridone-conjugated monobactam analogs with in vitro antibacterial activity against clinically relevant Gram-negative species including *Pseudomonas aeruginosa*, *Klebsiella pneumoniae* and *Escherichia coli*. Rat pharmacokinetic studies with compound **17** demonstrate low clearance and low plasma protein binding. In addition, evidence is provided for a number of analogs suggesting that the siderophore receptors PiuA and PirA play a role in drug uptake in *P.aeruginosa* strain PAO1.

INTRODUCTION

Infections caused by multidrug-resistant Gram-negative bacteria, particularly in the hospital setting, result in thousands of deaths per year and are the source of considerable concern in the

medical community[1]. One strategy to develop new antibacterial agents capable of eradicating these pathogens involves the so-called "Trojan Horse" approach wherein the bacterial iron acquisition system is utilized to deliver a drug to the periplasmic space, thus enabling target engagement and cell death[2]. We and others have exploited this strategy to identify monocarbams[3] such as **1** (MC-1)[4], monosulfactams such as **2** (BAL30072)[5] and monobactams[6] such as isoxazole **3**[7] (Figure 1). In compounds **1-3**, the presence of a pyridone moiety is critical to the active uptake process which likely involves drug interaction with one or more bacterial siderophore receptors (*vide infra*)[8]. Our initial report of pyridone-conjugated monobactam analogs exemplified by **3** highlighted the potential of the series to provide molecules with respectable in vitro and in vivo activity against Gram-negative pathogens, including some multidrug-resistant (MDR) strains. We describe herein a more chemically diverse set of analogs, the design of which benefited from cocrystal structures of several ring-opened β-lactams with *Pseudomonas aeruginosa* Penicillin Binding Protein 3 (*Pae*PBP3).

Figure 1. Recently reported pyridone-conjugated monocyclic β-lactams.

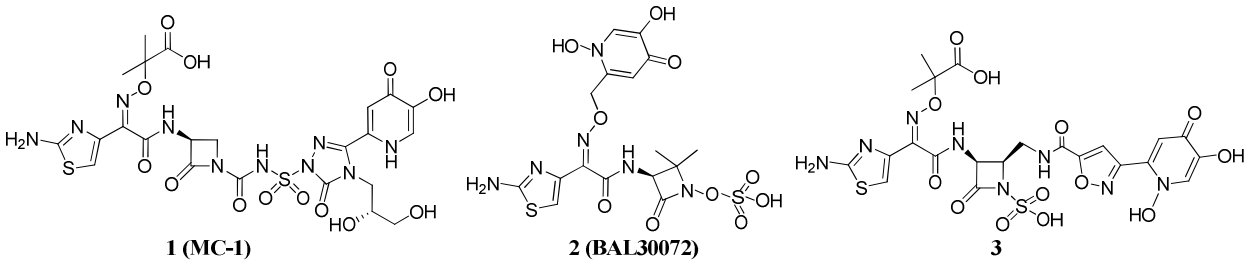

CHEMISTRY

Detailed experimental methods utilized in the preparation of all analogs, including the intermediates described below, are available in the Supporting Information. A number of analogs in Tables 1 and 4 were prepared as shown in Scheme 1. Enantiomer **4** was isolated from

the racemic-*cis* precursor[9] by use of chiral resolution via supercritical fluid chromatography. Ester reduction of **4** with $NaBH_4$ and removal of the CBZ protecting group by hydrogenolysis provided aminoalcohol **5**. Coupling of amine **5** with the activated ester **9**, which is derived from the corresponding carboxylic acid[10], provided alcohol **6**. The hydroxyl group of this versatile intermediate could be converted to the corresponding amine **7**, thus providing access to a variety of amino-linked compounds, including carbamate **8**. Lactam N-sulfation, typically with pyridine•SO_3, followed by global deprotection, typically with BCl_3, provided final analogs such as **18**.

Preparation of the pyridone intermediates utilized in the synthesis of final analogs were generally derived from kojic acid (**10**). For example, monoprotection of the phenolic oxygen of kojic acid with 4-methoxybenzyl chloride followed by heating with hydroxylamine and subsequent reaction with 4-methoxybenzyl chloride provided intermediate **11** which was utilized in the preparation of **18**. The pyridone-2-carboxylic acids utilized in the preparation of a number of analogs in Table 4 involved protection of the kojic acid phenol with a benzyl group followed by oxidation of the 2-hydroxymethyl moiety to a carboxylic acid with $NaClO_2$/TEMPO(cat)/bleach(cat)[11]. Reaction of this intermediate with the requisite amine then provided the pyridone-2-carboxylic acids **12**. Standard amide coupling methodology of **12** with amine **7** provided access to Table 4 analogs.

A number of the analogs with modified oxime substituents described in Tables 2 and 3 were prepared as shown in Scheme 2. Condensation of O-alkylhydroxylamines, such as **15**, with ketone **13** provided oxime acid **14**. Standard amide coupling with amine **16** (see Supplementary Information for preparation) followed by sulfation and global deprotection as described above provided final targets, such as **27**.

Scheme 1. Preparation of **18**.

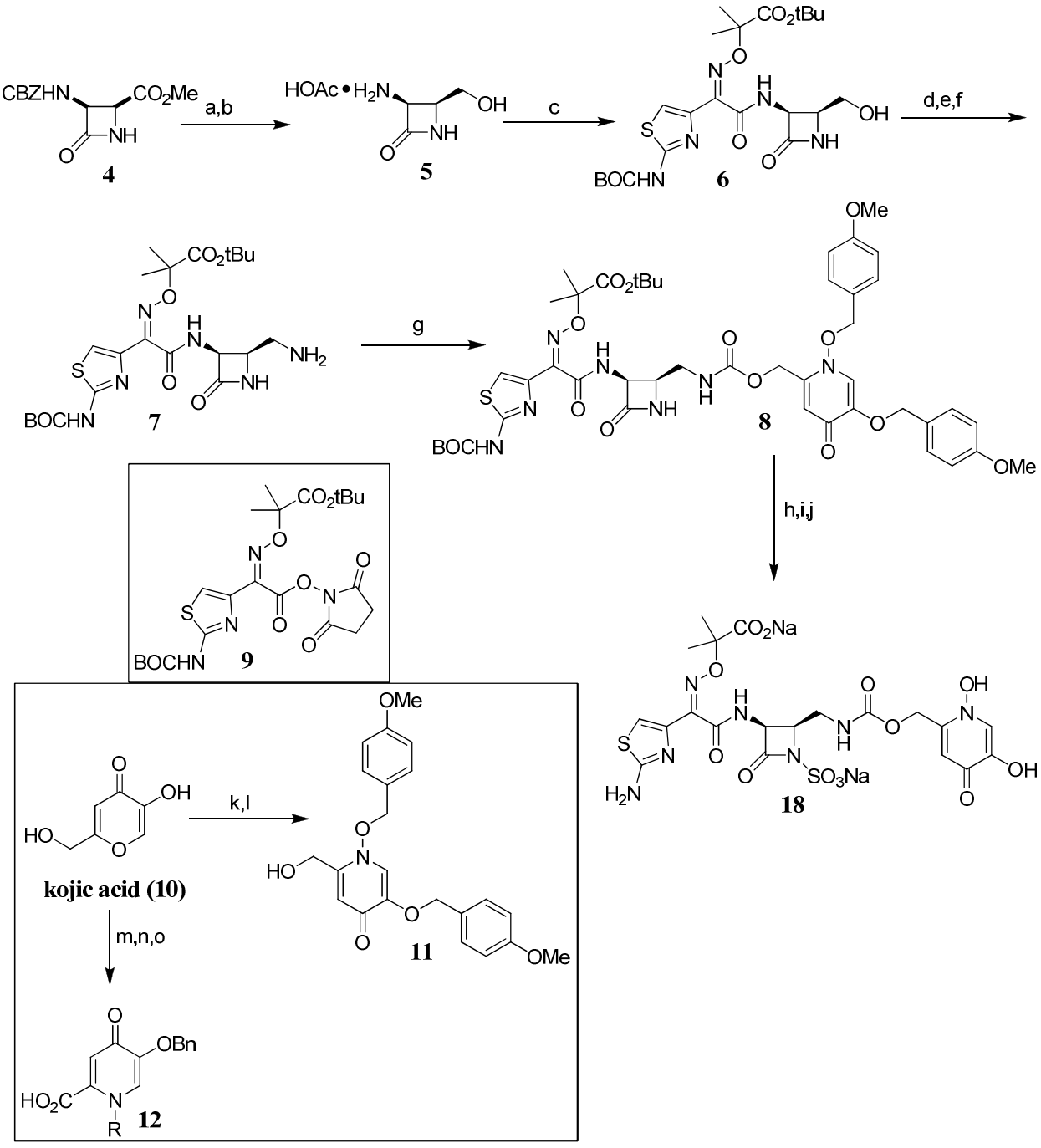

Reagents and conditions: (a) $NaBH_4$, MeOH, 20 °C; (b) 20% $Pd(OH)_2/C$, H_2 (50 psi), glacial HOAc, EtOH; (c) **9**, NEt_3, MeCN, RT; (d) PPh_3, imidazole, I_2, CH_2Cl_2, RT; (e) NBu_4N_3, NEt_3, 2-Me-THF; (f) 10% Pd/C, H_2 (30 psi), EtOH; (g) **11**, CDI, THF; (h) pyridine•SO_3, DMF, RT; (i)

BCl_3, CH_2Cl_2, RT; (j) $NaHCO_3$, water; (k) 4-methoxybenzyl chloride, NMP, K_2CO_3, 75 °C; (l) (i) NH_2OH•HCl, K_2CO_3, NMP, (ii) 4-methoxybenzyl chloride; (m) BnBr, NaOH, MeOH, reflux; (n) TEMPO, $NaClO_2$, NaClO, Na-phosphate buffer, CH_3CN, 35 °C; (o) RNH_2, MeOH, RT.

Scheme 2. Method for preparing oxime modified analogs.

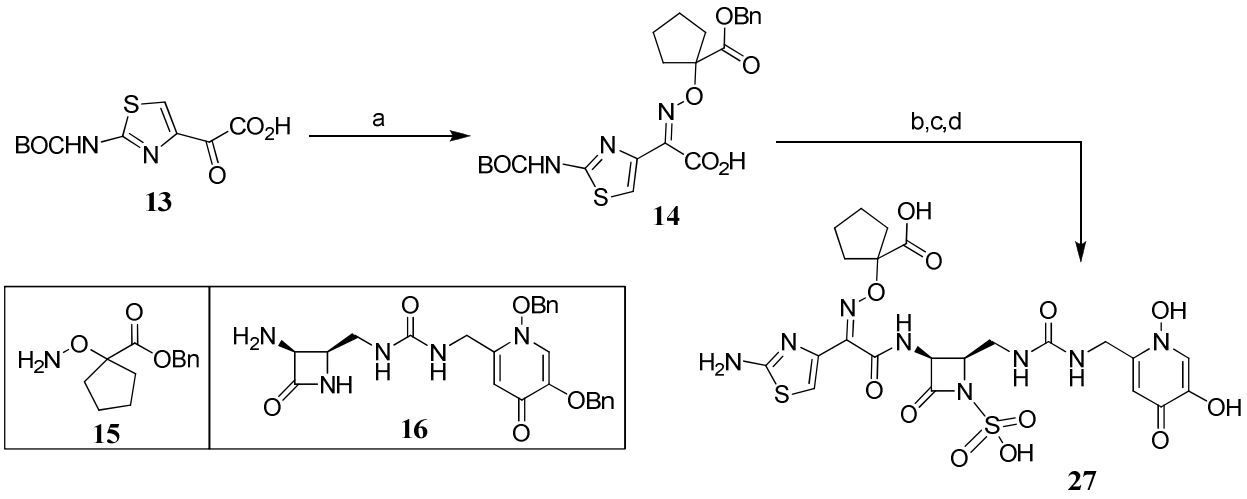

Reagents and conditions: (a) **15**, MeOH, RT; (b) **16**, HATU, $NaHCO_3$, DMF, RT; (c) pyridine•SO_3, DMF, RT; (d) BCl_3, CH_2Cl_2, RT.

RESULTS AND DISCUSSION

All analogs were screened for minimum inhibitory concentrations (MICs) against a primary panel of Gram-negative pathogens. The panel included strains susceptible to clinically relevant drugs as well as some with a MDR phenotype (Tables 1-4). For example, *P. aeruginosa* strain 1091-05 and *A. baumannii* strain AB-3167 are susceptible to antibacterial drugs from multiple classes while *K. pneumoniae* strain 1000-02 is aztreonam resistant and meropenem sensitive. *P. aeruginosa* strain 1042-06 and *K. pneumoniae* strain 1487-07 (KPC-2, TEM-1 and SHV-12) display moderate to high level resistance to all of the comparator agents.

The antibacterial mechanism of action of β-lactams involves acylation of an active site serine residue from one or more penicillin binding proteins (PBPs) leading to enzyme inactivation, which produces cell wall irregularities and ultimately, cell death. In general, monobactams, such as aztreonam and the compounds described below, are potent inhibitors of Gram-negative PBP3, display moderate PBP1a and 1b inhibition and no relevant PBP2 inhibitory activity (Table 8)[5a, 12]. Given the potent PBP3 inhibitory activity of this class, our initial structure based drug design efforts focused on understanding drug interactions with this enzyme. Indeed, a number of recent publications from our group describe cocrystal structures of ring-opened β-lactams bound to *Pae*PBP3 and this work contributed significantly to the design of novel analogs described below. For example, the x-ray structures of monocarbam **1** and monobactam **3** demonstrated that the linker motifs connecting the β-lactam cores to the pyridone moieties of both analogs occupy a fairly sizable tunnel defined, in part, by Val333 and Phe533[7, 13]. A similar binding mode is observed with the novel monobactam analog **17** bound to *Pae*PBP3, with the urea linker occupying this tunnel (Figure 2). Overall, this structural data suggests that a wide range of linker groups could be accommodated in this tunnel region, and indeed, a number of new compounds with potent anti-*pseudomonal* activity were discovered in this vein. For example, urea **17**, carbamate **18**, triazoles **20** and **21** and 2-aminopyridyl analog **22** displayed improved activity relative to the comparator agents against the drug resistant *P. aeruginosa* strain 1042-06. In addition, most analogs proved to be superior to the class-comparator aztreonam against the *K. pneumoniae* strain 1000-02 with a number of compounds matching the potency of meropenem (**17**, **20**, **21**). In addition, urea **17** was effective against the MDR KPC-harboring *K. pneumoniae* strain, 1487-07, and all analogs (and comparator drugs) in Table 1 provided moderately low MICs against the susceptible *A. baumannii* strain AB-3167. However, not all linkers provided

the desired level of potency and/or spectrum. For example, while urea **17** exhibited a promising profile, the closely related sulfamide **19** showed diminished potency in the primary panel relative to **17**, especially vs. the drug resistant strains 1042-06 and 1487-07 and the pyridyl-linked analog **22** displayed inferior activity vs. the *K. pneumoniae* strain 1487-07.

While the *Pae*PBP3 cocrystal structures catalyzed the design of the various linkers described above, the enhanced cellular potency of the analogs relative to aztreonam is not likely due to enhanced inhibition of PBP3. For example, compound **3** and aztreonam have similar enzyme IC_{50}s (Table 8), while urea **17** is approximately 10-fold less potent. Both **3** and **17** display improved PBP1a and 1b IC_{50}s relative to aztreonam, which, when combined with the siderophore uptake mechanism, likely explains the enhanced cellular potency of these analogs relative to aztreonam.

Figure 2. Cocrystal structure of **17** with *Pae*PBP3.

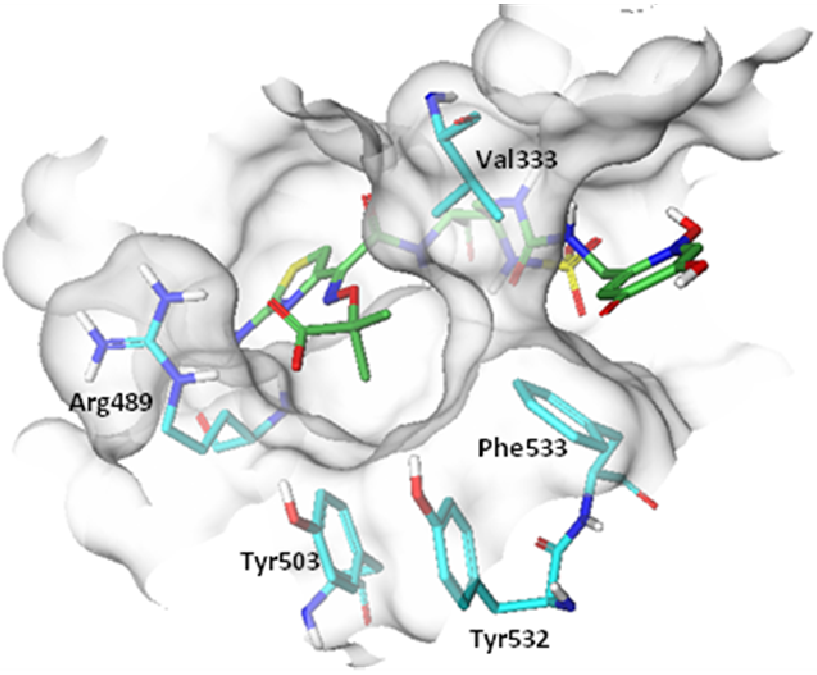

Table 1. C4 Linker modification.

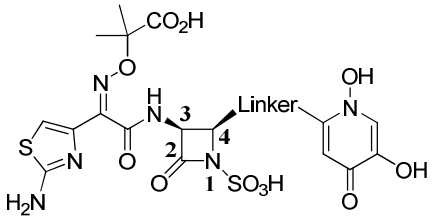

Cmpd	Linker	*P. aeruginosa* strains (μg/mL)		*K. pneumoniae* strains (μg/mL)		*A. baumannii* strain (μg/mL)
		1091-05	**1042-06**	**1000-02**	**1487-07**	**AB-3167**
aztreonam		4	64	>64	>64	4
cefepime		2	32	NT [a]	>64	2
meropenem		2	64	0.25	64	0.25
ciprofloxacin		0.125	64	NT	>64	0.06
amikacin		2	8	NT	64	1
3 [b]	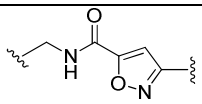	0.25	0.25	1	NT	0.125
17	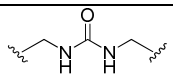	0.25	2	0.25	2	0.25
18 [b]	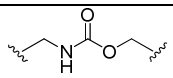	0.25	2	4	NT	0.125
19	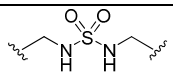	1	16	4	32	1
20	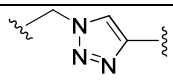	0.125	0.125	0.25	NT	0.125
21	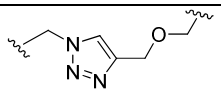	0.25	1	0.25	NT	0.25
22	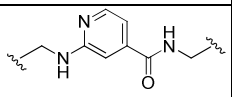	0.125	1	0.5	16	0.125

[a] NT = not tested

[b] bis-Na-salt

The β-lactam C3 carboxamide moiety in the analogs described above is found in a variety of β-lactam drugs (Figure 3). The recently published cocrystal structures of monocarbam **1**, aztreonam and ceftazidime with *Pae*PBP3 illustrate multiple productive drug-protein interactions with this sidechain and learnings from these structures laid the groundwork for C3 monobactam optimization efforts[13]. For example, in all cases, the *cis*-oxime linked gem-dimethyl group was found to interact with a hydrophobic pocket formed by Tyr503, Tyr532, Phe533 and Val333, and the carboxylic acid participates in a salt bridge interaction with Arg489. Analogous interactions are observed in the cocrystal structure of *Pae*PBP3 with urea **17** (Figure 2) and molecular modeling studies (see experimental section for model details) suggest that increasing the size of the gem-dialkyl group could potentially provide a better fit with the hydrophobic pocket described above. Dimethyl substitution (**17**) was roughly similar to the desmethyl analog **23** with regard to *P. aeruginosa* MICs, and somewhat improved relative to the mono-alkyl analogs **24** and **25** (Table 2). Constraining the gem dialkyl substituents via ring formation provided interesting SAR with the 4-membered ring analog **26** demonstrating roughly equivalent potency and spectrum as compared to the dimethyl analog **17**. Ring expansion to a cyclopentyl group (**27**) provided no additional benefit while incorporation of a cyclohexyl group (**28**) led to a 4 to 8-fold loss of potency across the primary strain set relative to the cyclobutyl analog **26**, thus providing some guidance regarding the preferred substituent size for this hydrophobic pocket. The similar *P. aeruginosa* MICs observed for **26** and **17** translated to PBP enzyme inhibitory activity as the two compounds display similar potencies against PBP3 as well as PBP1a, 1b and 3 (Table 8).

Figure 3. Selection of β-lactam drugs with similar carboxamide moieties.

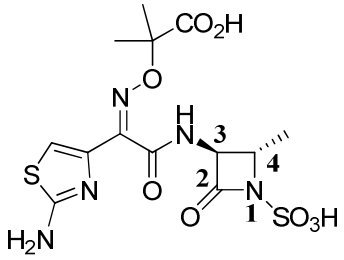

Aztreonam

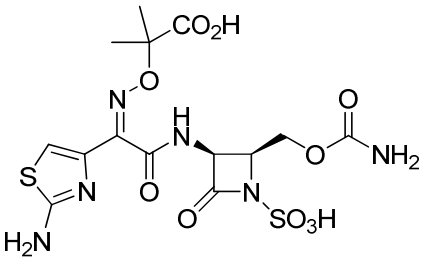

Tigemonam

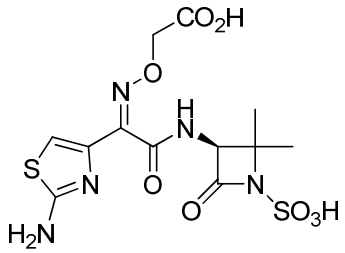

Carumonam

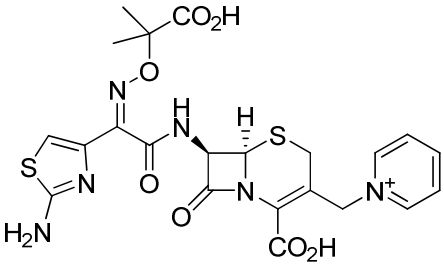

Ceftazidime

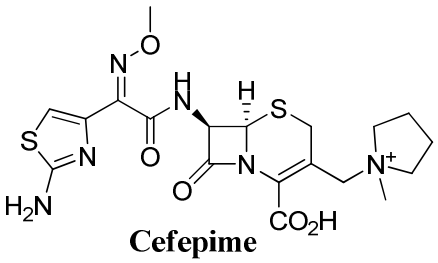

Cefepime

Table 2. Oxime group modifications of **17**.

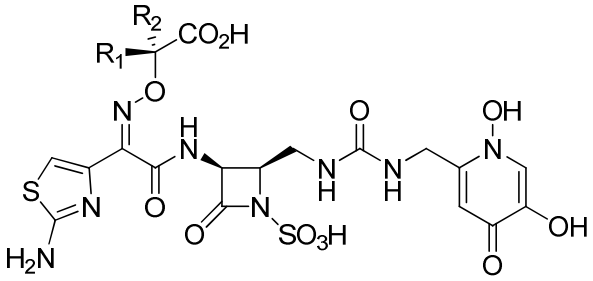

Cmpd	R1	R2	*P. aeruginosa* strains (μg/mL)		*K. pneumoniae* strains (μg/mL)		*A. baumannii* strain (μg/mL)
			1091-05	**1042-06**	**1000-02**	**1487-07**	**AB-3167**
aztreonam			4	64	>64	>64	4
cefepime			2	32	NT[a]	>64	2
meropenem			2	64	0.25	64	0.25
ciprofloxacin			0.125	64	NT	>64	0.06

amikacin			2	8	NT	64	1
17	Me	Me	0.25	2	0.25	2	0.25
23	H	H	0.125	4	1	8	0.25
24	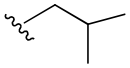	H	1	16	0.5	1	1
25	Bn	H	1	8	1	1	1
26	$-(CH_2)_3-$		0.125	1	0.125	0.5	0.125
27	$-(CH_2)_4-$		0.25	1	0.25	0.5	0.125
28	$-(CH_2)_5-$		1	8	0.5	4	1

[a] NT = not tested

Attempts to improve potency by modifying the *cis*-oxime substituent of compound **17** were generally unsuccessful (Table 3). For example, homologation (**29**) or isosteric replacement of the carboxylate with a tetrazole (**31**) led to a moderate loss of potency relative to **17** against the MDR *P. aeruginosa* strain 1042-06. Replacement of the carboxylate with a hydroxamic acid (**30**) led to a more pronounced loss of activity vs. 1042-06, and this is also reflected in the diminished PBP1a, 1b and 3 inhibitory activity of **30** relative to compound **17** (Table 8). Analogs with lipophilic moieties lacking the carboxylic acid, such as the phenyl- (**32**), cyclopentyl- (**33**) and thiazolyl-containing (**34**) compounds, were also inferior vs. 1042-06 as was replacement of the acid with either an alcohol (**35**) or amine (**36**). Comparison of cyclopentyl analog **33** with the analogous carboxylate-containing compound **27** demonstrates the contribution of the carboxylate-Arg489 salt-bridge interaction to potency, and the reduced activity of amine **36** is not surprising given the potential for charge repulsion with nearby Arg489. All analogs in this set were significantly less potent than **17** vs. both *K. pneumoniae* strains. Respectable activity is observed against the *A. baumannii* strain AB-3167, with MICs falling in the same range as that observed for the comparator drugs.

Table 3. Additional oxime modifications of **17**.

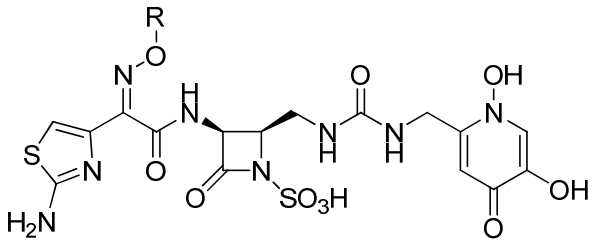

Cmpd	R	*P. aeruginosa* strains (μg/mL)		*K. pneumoniae* strains (μg/mL)		*A. baumannii* strain (μg/mL)
		1091-05	**1042-06**	**1000-02**	**1487-07**	**AB-3167**
aztreonam		4	64	>64	>64	4
cefepime		2	32	NT[a]	>64	2
meropenem		2	64	0.25	64	0.25
ciprofloxacin		0.125	64	NT	>64	0.06
amikacin		2	8	NT	64	1
17	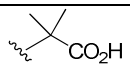	0.25	2	0.25	2	0.25
29	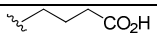	0.5	8	32	>64	0.5
30	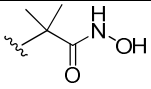	1	>64	8	16	1
31	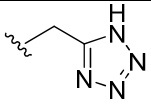	0.5	16	8	32	0.5
32	Ph	0.5	16	>64	>64	0.5
33	cyclopentyl	1	16	8	32	1

34	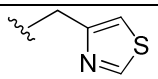	1	>64	16	16	1
35	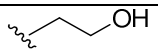	0.5	16	32	32	0.5
36	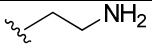	4	>64	>64	>64	4

[a] NT = not tested

Bacteria express a wide variety of siderophores and siderophore receptors, and as previously reported, uptake of **1** and **2** in *P. aeruginosa* strain PAO1 likely involves the siderophore receptors PiuA and PirA[8]. These receptors are known to be involved in recognition and uptake of bacterial catechol-containing siderophores, such as enterobactin[14]. Enterobactin is a well-characterized siderophore which is produced by *E. coli* and other *Enterobacteriaceae* and is utilized by a number of bacteria (including *P. aeruginosa*) to sequester iron[15]. One plausible theory regarding the cellular uptake of the monobactam analogs described here is that the pyridone moiety mimics the catechol groups found in enterobactin and related siderophores leading to receptor binding and delivery of drug to the bacterial periplasmic compartment. To explore the pyridone SAR, a variety of structurally similar analogs were prepared (Table 4). The N-unsubstituted (**37**) and N-hydroxy (**38**) pyridones displayed the best potency vs. both *P. aeruginosa* strains. In general, our experience across a range of monobactam analogs suggests that the N-hydroxy pyridone moiety present in compound **38** typically provides the best overall potency and spectrum. Moderate activity and spectrum was observed for a number of other analogs, including the N-methoxy (**39**), N-methyl (**40**), N-CH_2CO_2H (**41**) and N-NHMe (**43**) and significantly diminished potency and spectrum was observed for both the N-phenyl pyridone **42** and pyranone **44**, with **42** also demonstrating somewhat reduced PBP1b and 3 inhibitory activity (Table 8). It is interesting to note that compounds **45** and **46** retain structural features most

similar to the catechol moieties found in enterobactin, yet are the least active compounds in this set. Unfortunately, PBP enzyme inhibition data is not available for either analog, so we are unable to determine if the loss of cellular potency is due to reduced enzyme inhibition, reduced siderophore receptor-mediated cellular uptake, or a combination of both factors.

Table 4. Pyridone modification.

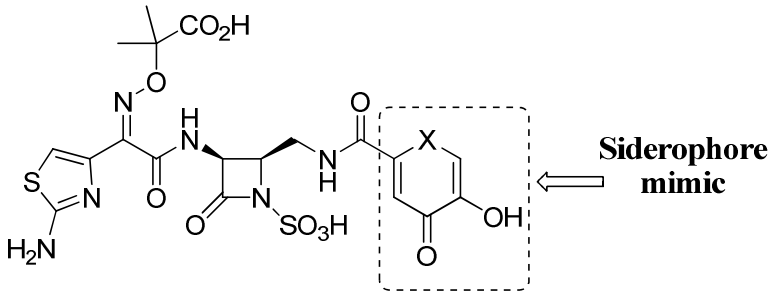

Cmpd	X	*P. aeruginosa* strains (μg/mL)		*K. pneumoniae* strains (μg/mL)		*A. baumannii* strain (μg/mL)
		1091-05	**1042-06**	**1000-02**	**1487-07**	**AB-3167**
aztreonam		4	64	>64	>64	4
cefepime		2	32	NT[a]	>64	2
meropenem		2	64	0.25	64	0.25
ciprofloxacin		0.125	64	NT	>64	0.06
amikacin		2	8	NT	64	1
37	NH	0.125	0.5	0.5	NT	0.125
38[b]	NOH	0.5	0.5	<0.06	0.25	0.5
39	NOMe	1	4	1	8	1
40	NMe	4	4	0.25	4	4

41	NCH_2CO_2H	1	2	0.25	4	1
42	NPh	32	32	1	16	32
43	NNHMe	2	8	0.5	8	2
44	O	8	64	32	64	8
	Siderophore mimic					
45	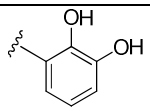	16	32	64	64	16
46	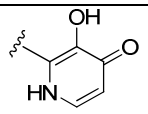	32	>64	32	64	32

[a] NT = not tested

[b] bis-Na-salt

Since compound **17** displayed good overall potency against the initial Gram-negative panel, it was further evaluated against a broader set of clinically relevant pathogens known to express a variety of resistance mechanisms (Table 5, SI1-SI9). As in Table 1, representatives from several drug classes are included for comparison. The majority of cystic fibrosis (CF) patients suffer chronic *P. aeruginosa* infections, requiring nearly continual antibiotic therapy[16]. When evaluated against a panel of 17 *P. aeruginosa* strains from CF patients, compound **17** provided superior $MIC_{50/90}$ values relative to the comparator drugs, and also performed well vs. 15 *P. aeruginosa* strains harboring metallo-β-lactamases[17] which showed high level resistance to all comparator drugs, except aztreonam. Meropenem proved superior to **17** in *K. pneumoniae*

panels expressing a variety of β-lactamases[17], the exception being a KPC-positive panel which exhibited high level resistance to all comparator drugs, but was moderately susceptible to compound **17**. Against several *E. coli* panels composed of a variety of β-lactamase producers, both **17** and meropenem consistently delivered low $MIC_{50}/_{90}$ values relative to the other comparator drugs. While good potency was observed for both **17** and comparator drugs against the susceptible *A. baumannii* strain AB-3167 (Table 1), no compound provided a low MIC_{90} against a collection of 31 clinical strains of *A. baumannii*, with meropenem and ciprofloxacin providing the best MIC_{50} values (1 and 0.5 μg/mL). The relatively poor performance of ciprofloxacin and amikacin against most panels described in Table 5 suggests the presence of one or more additional resistance mechanisms beyond the expression of β-lactamases. Examples could include upregulation of efflux pumps, downregulation of porin channels, drug target binding site mutations and expression of aminoglycoside-modifying enzymes.

Table 5. $MIC_{50}/_{90}$ data for compound **17** and comparator drugs.

Bacterial Strain (phenotype)	**# of strains tested**	**$MIC_{50}/_{90}$ (μg/mL)**					
		17	**Aztreonam**	**Cefepime**	**Meropenem**	**Ciprofloxacin**	**Amikacin**
P. aeruginosa (CF patients)	17	0.25/4	8/64	8/>64	1/16	2/16	8/>64
P. aeruginosa (metallo-β-lactamase)	15	0.25/1	8/16	>64/>64	>64/>64	32/>64	>64/>64
K. pneumoniae (ESBL)	17	0.125/1	32/>64	8/>64	0.03/0.25	0.25/>64	4/64

K. pneumoniae (defined β-lactamase)	30	0.5/16	64/>64	4/>64	0.03/0.25	0.5/64	4/>64
K. pneumoniae (KPC)	22	4/16	>64/>64	>64/>64	32/>64	64/>64	32/>64
E. coli (ESBL)	16	0.25/2	64/>64	64/>64	0.03/0.06	>64/>64	8/64
E. coli (defined β-lactamase)	18	0.125/1	4/>64	0.25/4	0.03/0.06	0.03/0.06	1/16
E. coli (CTX-M)	11	0.5/1	64/>64	64/>64	0.03/0.06	64/>64	8/32
Acinetobacter spp.	31	8/>64	32/>64	8/>64	1/32	0.5/>64	4/>64

In order to determine which bacterial siderophore receptors may be involved in drug uptake, monobactams **3**, **17** and **38** were evaluated against a panel of siderophore receptor-deficient *P. aeruginosa* strains. This panel was reported previously for determining the specific siderophore receptors utilized in the uptake of **1** and **2**[8]. No relevant MIC shift relative to the parent strain PAO1 was observed with **3**, **17** and **38** when evaluated against mutant strains lacking the receptors involved in uptake of the major *P. aeruginosa* siderophores pyoverdin (FpvA) and pyochelin (FptA) (Table 6). However, a significant (16- to 32-fold) shift in MIC was observed for the PiuA receptor-deficient strain relative to the parent strain when the assay utilized standard Mueller-Hinton broth (MHB). The MIC shift was much less pronounced when conducted in

modified low-iron MHB[8], supporting the notion that siderophore receptor expression is regulated by iron availability.[18] Evaluation of **3**, **17** and **38** vs. the Δ*pirA* single mutant strain in either normal or low-iron media showed no MIC shift, however, evaluation vs. the Δ*piuA*Δ*pirA* double mutant strain provided a ≥64-fold MIC shift relative to the parent strain for all compounds in both standard and low-iron media. This was the only example of a second mutation on the Δ*piuA* background which provided an additional MIC shift beyond that observed with the Δ*piuA* single mutant. This may suggest that PiuA is the dominant uptake receptor for these compounds in PAO1, while PirA functions as a secondary receptor whose expression is upregulated under low-iron conditions leading to enhanced drug uptake, thus explaining the reduced MIC shift for the Δ*piuA* mutant in low-iron vs. standard MHB media. These results are analogous to those reported previously for **1** and **2**[8] and may suggest a common uptake mechanism for pyridone-conjugated β-lactams.

Table 6. PAO1 isogenic siderophore receptor mutant panel.

	MIC (μg/mL)					
	3		**17**		**38**	
Strain	MHB[a]	Low-iron[b]	MHB	Low-iron	MHB	Low-iron
PAO1	0.25	0.25	0.25	0.125	0.5	0.5
piuA	8	1	8	0.5	8	0.5
pirA	0.25	0.25	0.25	0.25	0.5	0.5
fpvA	0.125	0.125	0.25	0.06	1	0.5
fptA	0.25	0.25	0.25	0.25	0.5	0.5
piuA fpvA	8	0.5	8	0.25	16	1
piuA fptA	8	1	8	0.5	8	0.5

piuA pirA	32	16	32	32	64	64

[a] Mueller Hinton Broth.

[b] Iron-chelated version of MHB[8].

Plasma protein binding and rat pharmacokinetic studies were conducted with a subset of analogs to enable compound selection for advanced studies, and Table 7 provides representative data for urea **17**, carbamate **18** and triazole **21**. All three compounds exhibited relatively low binding to human, rat and mouse plasma proteins. Compounds **17** and **18** showed low plasma clearance in rat following iv dosing, while triazole **21** was cleared more rapidly, and this was especially apparent when comparing clearance values adjusted for protein binding and blood flow (Cl,int). A previous report from our group demonstrated a positive correlation between Cl,int and observed efficacy for related monobactams evaluated in a murine infection model,[7] supporting the selection of **17** for in vivo efficacy studies which will be reported in a future manuscript.

Table 7. Pharmacokinetic and protein binding data.

Cmpd	**Plasma Protein Binding f_u**			**Rat Plasma Clearance (mL/min/kg)**	**Rat Cl,int (ml/min/kg)[a]**
	Human	**Rat**	**Mouse**		
17	1.0 ± 0.29	0.91 ± 0.07	0.91 ± 0.07	8.4 ± 0.4	10 ± 0.5
18	0.51 ±0.06	0.61 ± 0.04	0.72 ± 0.03	14.2 ± 5.6	29 ± 15
21	0.50 ± 0.06	0.60 ± 0.07	0.80 ± 0.03	31.3 ± 0.4	94 ± 2.8

[a] Total plasma clearance corrected for protein binding and rat blood flow.

Table 8. *P. aeruginosa* Penicillin binding protein IC_{50}s.

Cmpd	IC_{50} (μM)			
	PBP1a	PBP1b	PBP2	PBP3
aztreonam	3.34 ± 0.57	2.87 ± 0.64	> 300	0.008 ± 0.004
3	0.11 ± 0.14	0.15 ± 0.13	> 300	0.006 ± 0.004
17	0.62 ± 1.0	1.67 ± 3.11	> 300	0.054 ± 0.044
26	0.34 ± 0.096	2.46 ± 0	> 300	0.066 ± 0.034
30[a]	3.02	11.1	> 300	0.27
42	0.58 ± 0.29	7.40 ± 0	> 300	0.14 ± 0

[a]n = 1 data.

In summary, we have described a structurally diverse collection of pyridone-conjugated monobactams with in vitro activity against a variety of clinically relevant Gram-negative pathogens. $MIC_{50/90}$ profiling of compound **17** demonstrated balanced antibacterial activity against a panel of *P. aeruginosa*, *K. pneumoniae* and *E. coli* strains harboring resistance mechanisms for a number of drug classes, including β-lactams, fluoroquinolones and aminoglycosides. Cocrystal structures of β-lactam ring-opened compounds, such as **17**, bound to *P. aeruginosa* PBP3 enzyme provided insight into drug-protein interactions and aided in the design of analogs described here. In addition, utilization of siderophore receptor knockout strains provided evidence suggesting involvement of the siderophore receptors PiuA and PirA in drug uptake in the *P. aeruginosa* strain, PAO1. Finally, rat PK studies conducted with urea **17** demonstrated low unbound clearance, supporting advancement of this analog to in vivo efficacy studies, the results of which will appear in due course.

EXPERIMENTAL SECTION

The experimental methods utilized to generate the *P. aeruginosa* siderophore receptor KO data have been described previously[8]. The minimum inhibitory concentration (MIC) values were determined using the broth microdilution protocol according to the methods of the Clinical and Laboratory Standards Institute (CLSI)[19]. Plasma protein binding values were determined using a modification of a reported method[20]. The assay was conducted at ambient temperature rather than 37 °C. Positive controls were utilized for the protein binding studies; phenytoin was used for compound **17** and sertraline was utilized for compounds **18** and **21** and in all cases, acceptable positive control results were obtained relative to historical data.

***P. aeruginosa* PBP IC_{50} assay**. Membrane preparation (ATCC27853) was conducted according to a published method[21]. Membrane samples (75 μg) were mixed with 1.5 μL 100 μM EDTA, and the total volume of the resulting mixture was brought to 15 μL with PBS. The β-lactams tested were diluted in a 1 to 3 scheme in 1.5% DMSO so that 5 μL would give a final concentration of 300 μM to 0.005 μM (11 wells serially diluted 1 to 3 including a no compound control) in a 25 μL final assay volume. Samples were incubated at 35 °C for 20 minutes, followed by the addition of 5 μL of the fluorescent penicillin Bocillin FL (Molecular Probes, Inc.) suspended in PBS to yield a final assay concentration of 0.65 μM. Reaction mixtures were incubated at 35 °C for 20 min, then terminated by the addition of 25 μL 2× Laemmli buffer. After boiling in a water bath for 4 minutes, samples were centrifuged at 14,000 rpm for 2 minutes, and 10 μL was loaded onto a 10% Tris/Bis SDS gel (NuPage) run with the MES buffer system (Invitrogen) at 150 V for 75 min. The gel was washed briefly in deionized H_2O and scanned by a Storm 860 (Molecular Dynamics) at an excitation wavelength of 450 nm and an emission wavelength of 520 nm. An IC_{50} was determined for each β-lactam assayed

(concentration where the β-lactam causes a 50% reduction of the Bocillin FL binding to each PBP in the *P. aeruginosa* total membrane preparation).

Rat pharmacokinetic studies. All animal care and in vivo procedures conducted were in accordance with guidelines of the Pfizer Animal Care and Use Committee. Male Wistar Han rats (~250g) were housed one per cage in an American Animal Association Laboratory Animal Care accredited facility. This investigation conformed to the Guide for the Care and Use of Laboratory Animals published by the US National Institutes of Health (NIH Publication No. 85-23, revised 1996). Animals were allowed ad libitum access to water and food. Compounds were administered intravenously via the jugular vein cannula (n = 2), and were administered at 1.0 mg/kg i.v.. Compounds were formulated as a solution in 20 mM phosphate buffer (pH = 6). After dosing, serial plasma samples were collected at appropriate times and kept frozen at −20 °C until LC-MS/MS analysis.

LC-MS/MS method. A non-validated liquid chromatography-tandem mass spectrometry (LC-MS/MS) was used to determine compound concentrations in the plasma protein binding and rat pharmacokinetic assays. Samples were injected (10 mL) onto a Phenomenex Monolithic C18 column (5 mm, 50 x 2.0 mm). The column was equilibrated with mobile phase (A: 0.1% formic acid in water / B: 0.1% formic acid in acetonitrile) at a flow rate of 0.8 mL/min. The gradient started at 0% B and was ramped to 95% B from 0.0 to 0.6 min, then returned to starting conditions by 0.9 min and held for an additional 0.6 min for a total run time of 1.5 min. The effluent was analyzed by a mass spectrometer detector (AB Sciex API-4000), fitted with a turbo ion spray interface and operated in positive ion mode. Aztreonam was used as the internal standard for both protein binding and rat PK studies.

Molecular Modeling. β-lactam ring-opened models of pyridone-conjugated monobactam analogs bound to *Pae*PBP3 were generated using the following procedure. The 2D structures of the closed form of the compounds were converted into single low energy 3D conformations using Corina[22]. Protons were titrated appropriately at pH = 7.4 using an internal software CVT[23]. Multiple low energy conformations (maximum number of conformations = 100) of the compounds were generated using Omega[24]. A shape-based matching protocol to select the conformation most similar to the closest crystal structure was then performed using ROCS[25]. This was taken as the initial pose in the binding site, which was then refined by an "in-situ" bond clipping of the β-lactam in the enzyme active site followed by minimizing the compound in the context of the protein using Macromodel[26] and the OPLS2005 force field[27]. Exhaustive conformational searching using the Monte-Carlo Multiple Minimization (MCMM) algorithm was implemented in MacroModel and the 10 lowest minimum energy conformations were visually inspected to select a reasonable, representative binding conformation.

Chemistry. A purity of ≥ 95% as determined by either HPLC or LCMS was achieved for all final analogs, with the exception of compounds **19** (88%, HPLC), **22** (88%, HPLC), **23** (92%, HPLC), **32** (88%, HPLC), **35** (92%, HPLC), **36** (90%, HPLC), **37** (>90%, HPLC) and **34** (94%, HPLC). The synthesis of compound **18** is provided below. Detailed synthetic procedures and spectral characterization for all compounds is provided in the Supporting Information.

Sodium 2-((Z)-1-(2-aminothiazol-4-yl)-2-((2R,3S)-2-((((1,5-dihydroxy-4-oxo-1,4-dihydropyridin-2-yl)methoxy)carbonylamino)methyl)-4-oxo-1-sulfonatoazetidin-3-ylamino)-2-oxoethylideneaminooxy)-2-methylpropanoate (18).

(2S,3S)-Methyl 3-(benzyloxycarbonylamino)-4-oxoazetidine-2-carboxylate (4). Chiral resolution of racemic-*cis*-**4**[9] was achieved by supercritical fluid chromatography (Chiralcel OJ-H: CO_2 / propanol) to afford **4** as a white solid. For literature characterization of **4**, see Y. Takahashi, *et al*.[28] 99.7% ee. LCMS *m/z* 279.2 (M+1). $[\alpha]^{20}$ +81.93° (*c* 0.035, $CHCl_3$). ^{1}H NMR (400 MHz, DMSO-d_6) δ 8.60 (br s, 1H), 8.14 (d, *J*=8.8 Hz, 1H), 7.34-7.29 (m, 5H), 5.05-5.01 (m, 3H), 4.35 (d, *J*=5.5 Hz, 1H), 3.53 (s, 3H).

(3S,4S)-3-Amino-4-(hydroxymethyl)azetidin-2-one (HOAc salt) (5). A solution of **4** (72.5 g, 260 mmol) in methanol (725 mL) at 20 °C was treated with a suspension of sodium borohydride (18.7 g, 495 mmol) in isopropyl alcohol (145 mL) added portionwise over 30 minutes, the temperature was maintained between 26-33 °C. The reaction mixture was stirred for 20 minutes. The methanol was removed in vacuo and the mixture was treated with brine solution (200 mL) and water (200 mL). The white slurry was extracted with ethyl acetate (700 mL) and washed with brine solution (3 x 200 mL). The aqueous layer was back extracted with ethyl acetate / isopropyl alcohol (10:1, 2 x 220 mL) and the combined organic layers were dried over magnesium sulfate. The suspension was filtered under vacuum and the filtrate concentrated in vacuo to give crude material (81.2 g) as a solid. The crude material was treated with ethyl acetate (400 mL) followed by Darco KB (2 g) and Celite (5 g) and the mixture was stirred at room temperature for 30 minutes. The mixture was filtered and the solids washed with ethyl acetate (100 mL). The filtrate was treated with heptane (750 mL) over 30 minutes. The white slurry was filtered and the solid washed with ethyl acetate / heptane (2 : 3, 150 mL) to afford benzyl (2S,3S)-2-(hydroxymethyl)-4-oxoazetidin-3-ylcarbamate as a white solid. Yield: 59.3 g, 237 mmol, 91%. LCMS *m/z* 251.6 (M+1). $[\alpha]^{20}$ +9.03° (*c* 0.064, $CHCl_3$). mp 125-127 °C. ^{1}H

NMR (400 MHz, $CDCl_3$) δ 7.35-7.28 (m, 5H), 5.67 (br s, 1H), 6.18 (d, *J*=9.9 Hz, 1H), 5.15 (dd, *J*=9.8, 4.8 Hz, 1H), 5.08 (s, 2H), 3.85-3.79 (m, 2H), 3.65 (m, 1H), 3.36 (br s, 1H).

To a solution of benzyl (2S,3S)-2-(hydroxymethyl)-4-oxoazetidin-3-ylcarbamate (29.4 g, 117.6 mol) in ethanol (589 mL) was added 9.0 g of Darco (Norit KB). The resulting slurry was stirred for 1 hour and the Darco was removed by vacuum filtration, then the Darco cake was rinsed with ethanol (294 mL). The ethanolic filtrate was treated with glacial acetic acid (13.5 mL, 236 mmol) and the resulting mixture was charged with 5.9 g of 20% palladium hydroxide. The mixture was purged with nitrogen followed by hydrogen and pressurized to 50 psi hydrogen. The reaction mixture was agitated at 25 °C for 16 hours. The mixture was filtered and the filter cake was rinsed with ethanol (150 mL). The ethanolic filtrate was concentrated to afford **5** as an oil. Yield: 26.82 g, 152.2 mmol, >100%. ^{1}H NMR (400 MHz, CD_3OD) δ 4.29 (d, *J*=4.8 Hz, 1H), 3.89 (dd, *J*=13.0, 4.8 Hz, 1H), 3.76-3.81 (m, 2H), 1.98 (s, 3H).

tert-Butyl 2-((Z)-1-(2-(tert-butoxycarbonylamino)thiazol-4-yl)-2-((2S,3S)-2-(hydroxymethyl)-4-oxoazetidin-3-ylamino)-2-oxoethylideneaminooxy)-2-methylpropanoate (6). A flask charged with **5** (26.82 g) was treated with a solution of (Z)-tert-butyl 2-(1-(2-(tert-butoxycarbonylamino)thiazol-4-yl)-2-(2,5-dioxopyrrolidin-1-yloxy)-2-oxoethylideneaminooxy)-2-methylpropanoate (**9**) (41.5 g, 78.81 mmol) in acetonitrile (200 mL), followed by triethylamine (55.0 mL, 394.6 mmol) added over 5 minutes. The reaction mixture was stirred for 16 hours. The solution was concentrated in vacuo to yield a yellow glass. The glass was dissolved in methyl *tert*-butyl ether (500 mL) and washed with water (1 x 250 mL), saturated aqueous sodium bicarbonate solution (1 x 250 mL), saturated brine solution (1 x 250 mL), 1% aqueous potassium carbonate solution (1 x 500 mL) and saturated brine solution (1 x 500 mL). The methyl *tert*-butyl ether organic layer was concentrated in vacuo to give crude material (38.0 g) as an off-

white solid. The crude material (38.0 g) was treated with acetone (95 mL) and heptane (285 mL). The mixture was heated to 45 °C and was held at this temperature for 30 minutes. The thin slurry was cooled to 20 °C and stirred for 16 hours. The off-white solids were collected by vacuum filtration and the isolated filter cake was washed with 25% acetone - heptane (100 mL) to afford a white solid. The solid was dried in a vacuum oven at 30 °C to afford **6**. Yield: 23.13 g, 43.8 mmol, 56%. LCMS *m/z* 528.1 (M+1). ^{1}H NMR (400 MHz, $CDCl_3$) δ 8.80 (br s, 1H), 8.02 (d, *J*=7.7 Hz, 1H), 7.31 (s, 1H), 6.48 (br s, 1H), 5.44 (br dd, *J*=7.7, 4.8 Hz, 1H), 4.30-4.36 (m, 1H), 4.02-4.06 (m, 1H), 3.84-3.89 (m, 2H), 1.57 (s, 3H), 1.55 (s, 3H), 1.53 (s, 9H), 1.45 (s, 9H).

tert-Butyl 2-((Z)-2-((2R,3S)-2-(aminomethyl)-4-oxoazetidin-3-ylamino)-1-(2-(tert-butoxycarbonylamino)thiazol-4-yl)-2-oxoethylideneaminooxy)-2-methylpropanoate (7). To a solution of **6** (10.0 g, 18.9 mmol) in anhydrous dichloromethane (100 mL) at 20 ^{o}C under nitrogen was added triphenylphosphine (10.0 g, 38 mmol), followed by imidazole (2.58 g, 38 mmol). The reaction mixture was treated with iodine (9.62 g, 38 mmol) in portions over 10 minutes. The solution was allowed to warm to 20 ^{o}C and stirring was continued for 15 hours. The reaction mixture was washed with saturated aqueous sodium thiosulfate (100 mL) and the aqueous layer was extracted with dichloromethane (2 x 100 mL). The combined organic layers were washed with brine solution (100 mL), dried over sodium sulfate, filtered under vacuum and the filtrate was concentrated in vacuo to give crude material (24 g) as an orange foam. The orange foam was purified by chromatography on silica gel (heptane /ethyl acetate 30 to 80%) to afford tert-butyl 2-((Z)-1-(2-(tert-butoxycarbonylamino)thiazol-4-yl)-2-((2S,3S)-2-(iodomethyl)-4-oxoazetidin-3-ylamino)-2-oxoethylideneaminooxy)-2-methylpropanoate as a white foam. Yield: 9.41 g, 14.8 mmol, 78%. LCMS *m/z* 638.0 (M+1). ^{1}H NMR (400 MHz, DMSO-d_6) δ

11.83 (br s, 1H), 9.24 (d, *J*=9.0 Hz, 1H), 8.71 (br s, 1H), 7.29 (d, *J*=0.8 Hz, 1H), 5.17 (ddd, *J*=9.0, 4.9, 1.7 Hz, 1H), 4.11 (ddd, *J*=10.6, 4.8, 3.7 Hz, 1H), 3.28 (dd, *J*=10.4, 3.6 Hz, 1H), 3.17 (dd, *J*=10.5, 10.4 Hz, 1H), 1.46 (s, 9H), 1.42 (s, 3H), 1.40 (s, 12H).

A solution of tert-butyl 2-((Z)-1-(2-(tert-butoxycarbonylamino)thiazol-4-yl)-2-((2S,3S)-2-(iodomethyl)-4-oxoazetidin-3-ylamino)-2-oxoethylideneaminooxy)-2-methylpropanoate (6.3 g, 9.88 mmol) in 2-methyltetrahydrofuran (60 mL) under nitrogen at 20 ^{o}C was treated with triethylamine (2.75 mL, 19.76 mmol), followed by dropwise addition of a 15% solution of tetrabutylammonium azide in tetrahydrofuran (22.49 g, 11.86 mmol). The reaction mixture was stirred at 20 ^{o}C for 2 hours, and then heated at 35 ^{o}C and stirred for 15 hours. The solution was cooled to room temperature, filtered under vacuum, the white solid was washed with methyl *tert*-butyl ether (2 x 100 mL), the filtrate was collected and the solvent was removed in vacuo to give a foam. The foam was dissolved in methyl *tert*-butyl ether (200 mL), washed with water (2 x 100 mL), brine solution (100 mL), dried over sodium sulfate, and filtered under vacuum. The filtrate was collected and concentrated in vacuo to afford a foam. The foam was dissolved in acetonitrile and concentrated (3 x 15 mL) and the residue was held under high vacuum to give tert-butyl 2-((Z)-2-((2R,3S)-2-(azidomethyl)-4-oxoazetidin-3-ylamino)-1-(2-(tert-butoxycarbonylamino)thiazol-4-yl)-2-oxoethylideneaminooxy)-2-methylpropanoate as a yellow foam. Yield: 5.24 g, 9.48 mmol, 96%. LCMS *m/z* 553.1 (M+1). ^{1}H NMR (400 MHz, DMSO-d_6) δ 11.82 (br s, 1H), 9.19 (d, *J*=8.9 Hz, 1H), 8.67 (br s, 1H), 7.28 (s, 1H), 5.24 (ddd, *J*=8.7, 5.1, 1.4 Hz, 1H), 3.89-3.95 (m, 1H), 3.64 (dd, *J*=12.9, 3.9 Hz, 1H), 3.39 (dd, *J*=12.9, 8.9 Hz, 1H), 1.46 (s, 9H), 1.44 (s, 3H), 1.42 (s, 3H), 1.40 (s, 9H).

A Parr shaker vessel was charged with tert-butyl 2-((Z)-2-((2R,3S)-2-(azidomethyl)-4-oxoazetidin-3-ylamino)-1-(2-(tert-butoxycarbonylamino)thiazol-4-yl)-2-

oxoethylideneaminooxy)-2-methylpropanoate (14.37 g, 26.0 mmol) and ethanol (140 mL). The mixture was purged with nitrogen and then treated with 10% palladium on carbon (5.7 g) and pressurized to 30 psi hydrogen. The reaction mixture was agitated at room temperature for 4 hours. The solution was filtered through a micro filter and the solvent was removed in vacuo to afford **7** as a brown solid. Yield: 13.22 g, 25.1 mmol, 97%. LCMS *m/z* 527.1 (M+1). ^{1}H NMR (400 MHz, DMSO-d_6) δ 9.1-9.3 (v br s, 1H), 8.25 (br s, 1H), 7.26 (s, 1H), 5.17 (d, *J*=4.9 Hz, 1H), 3.65 (ddd, *J*=6, 6, 5 Hz, 1H), 2.78 (dd, *J*=13.4, 5.8 Hz, 1H), 2.62 (dd, *J*=13.4, 6.3 Hz, 1H), 1.46 (s, 9H), 1.43 (s, 3H), 1.41 (s, 3H), 1.39 (s, 9H).

tert-Butyl 2-((Z)-2-((2R,3S)-2-((((1,5-bis(4-methoxybenzyloxy)-4-oxo-1,4-dihydropyridin-2-yl)methoxy)carbonylamino)methyl)-4-oxoazetidin-3-ylamino)-1-(2-(tert-butoxycarbonylamino)thiazol-4-yl)-2-oxoethylideneaminooxy)-2-methylpropanoate (8). A solution of 2-(hydroxymethyl)-1,5-bis(4-methoxybenzyloxy)pyridin-4(1H)-one (**11**) (see Supplementary Information for preparation) (300 mg, 0.755 mmol) in tetrahydrofuran (10 mL) was treated with 1,1'-carbonyldiimidazole (379 mg, 2.26 mmol) at room temperature and stirred for 20 hours. The yellow reaction mixture was treated with a solution of **7** (286 mg, 0.543 mmol) in tetrahydrofuran (25 mL). The mixture was stirred for 6 hours at room temperature, then treated with water (20 mL) and extracted with ethyl acetate (3 x 25 mL). The combined organic layers were dried over sodium sulfate, filtered and concentrated in vacuo. The crude material was purified via chromatography on silica gel (heptane / ethyl acetate / 2-propanol) to afford **8** as a light yellow solid. Yield: 362 mg, 0.381 mmol, 62%. LCMS *m/z* 950.4 (M+1). ^{1}H NMR (400 MHz, DMSO-d_6), characteristic peaks: δ 9.31 (d, *J*=8.4 Hz, 1H), 8.38 (s, 1H), 8.00 (s, 1H), 7.41 (br d, *J*=8.2 Hz, 2H), 7.36 (br d, *J*=8.8 Hz, 2H), 7.26 (s, 1H), 6.10 (s, 1H), 5.20 (s, 2H), 4.92 (br s, 4H), 3.77 (s, 3H), 3.76 (s, 3H), 1.45 (s, 9H), 1.38 (s, 9H).

(Z)-tert-Butyl 2-(1-(2-(tert-butoxycarbonylamino)thiazol-4-yl)-2-(2,5-dioxopyrrolidin-1-yloxy)-2-oxoethylideneaminooxy)-2-methylpropanoate (9). 1-Hydroxypyrrolidine-2,5-dione (8.84 g, 76.8 mmol) was added to a suspension of (Z)-2-(1-tert-butoxy-2-methyl-1-oxopropan-2-yloxyimino)-2-(2-(tert-butoxycarbonylamino)thiazol-4-yl)acetic acid[10] (30 g, 70 mmol) in dichloromethane (400 mL). The mixture was cooled to 0 °C, *N,N'*-dicyclohexylcarbodiimide (97%, 15.6 g, 73.3 mmol) was added, and the reaction was stirred at 0 °C for 30 minutes and then at room temperature for 3 hours. The mixture was filtered through Celite and concentrated in vacuo to afford **9** as a colorless solid. Yield: 36.17 g, 68.7 mmol, 98%. LCMS *m/z* 527.2 (M+1). ^{1}H NMR (400 MHz, $CDCl_3$) δ 8.31 (br s, 1H), 7.50 (s, 1H), 2.91 (br s, 4H), 1.61 (s, 6H), 1.54 (s, 9H), 1.43 (s, 9H).

2-((Z)-1-(2-Aminothiazol-4-yl)-2-((2R,3S)-2-((((1,5-dihydroxy-4-oxo-1,4-dihydropyridin-2-yl)methoxy)carbonylamino)methyl)-4-oxo-1-sulfoazetidin-3-ylamino)-2-oxoethylideneaminooxy)-2-methylpropanoic acid (18). A solution of **8** (181 mg, 0.191 mmol) in anhydrous *N,N*-dimethylformamide (2.0 mL) was treated with sulfur trioxide pyridine complex (302 mg, 1.91 mmol). The reaction mixture was allowed to stir at room temperature for 6 hours, then cooled to 0 °C and quenched with water. The resulting solid was collected by filtration and dried in vacuo to yield (2R,3S)-2-((((1,5-bis(4-methoxybenzyloxy)-4-oxo-1,4-dihydropyridin-2-yl)methoxy)carbonylamino)methyl)-3-((Z)-2-(1-tert-butoxy-2-methyl-1-oxopropan-2-yloxyimino)-2-(2-(tert-butoxycarbonylamino)thiazol-4-yl)acetamido)-4-oxoazetidine-1-sulfonic acid as a white solid. Yield: 145 mg, 0.14 mmol, 74%. APCI *m/z* 1028.5 (M-1). ^{1}H NMR (400 MHz, DMSO-d_6), characteristic peaks: δ 11.65 (br s, 1H), 9.37 (d, *J*=8.6 Hz, 1H), 8.87 (s, 1H), 7.49 (br d, *J*=8.6 Hz, 2H), 7.43 (br d, *J*=8.6 Hz, 2H), 7.26 (s, 1H), 7.01 (br d, *J*=8.9 Hz, 2H), 7.00 (br d, *J*=8.8 Hz, 2H), 5.43 (s, 2H), 5.20 (dd, *J*=8.4, 6 Hz, 1H),

4.01-4.07 (m, 1H), 3.78 (s, 3H), 3.77 (s, 3H), 3.50-3.58 (m, 1H), 3.29-3.37 (m, 1H), 1.44 (s, 9H), 1.37 (s, 9H).

A solution of (2R,3S)-2-((((1,5-bis(4-methoxybenzyloxy)-4-oxo-1,4-dihydropyridin-2-yl)methoxy)carbonylamino)methyl)-3-((Z)-2-(1-tert-butoxy-2-methyl-1-oxopropan-2-yloxyimino)-2-(2-(tert-butoxycarbonylamino)thiazol-4-yl)acetamido)-4-oxoazetidine-1-sulfonic acid (136 mg, 0.132 mmol) in anhydrous dichloromethane (5 mL) was treated with 1 M boron trichloride in *p*-xylenes (0.92 mL, 0.92 mmol) and allowed to stir at room temperature for 40 minutes. The reaction mixture was cooled in an ice bath, quenched with water (0.4 mL), and transferred into a solution of methyl *tert*-butyl ether : heptane (1:2, 12 mL). The solvent was removed in vacuo and the crude product was purified via reverse phase chromatography (C-18 column; acetonitrile / water gradient with 0.1% formic acid modifier) to yield **18** as a light yellow solid. Yield: 43 mg, 0.068 mmol, 51%. LCMS *m/z* 634.4 (M+1). ^{1}H NMR (400 MHz, DMSO-d_6), characteristic peaks: δ 9.29 (d, *J*=8.5 Hz, 1H), 8.10 (s, 1H), 7.04-7.10 (m, 1H), 7.00 (s, 1H), 6.75 (s, 1H), 5.05-5.30 (m, 3H), 4.00-4.07 (m, 1H), 1.42 (s, 3H), 1.41 (s, 3H).

18-Bis Na salt. A suspension of **18** (212 mg, 0.33 mmol) in water (10 mL) was cooled to 0 ^{o}C and treated with a solution of sodium bicarbonate (56.4 mg, 0.67 mmol) in water (2 mL), added dropwise. The reaction mixture was cooled to -70 ^{o}C (frozen) and lyophilized to afford **18-Bis Na salt** as a white solid. Yield: 210 mg, 0.31 mmol, 93%. LCMS *m/z* 632.5 (M-1). ^{1}H NMR (400 MHz, D_2O) δ 7.87 (s, 1H), 6.94 (s, 1H), 6.92 (s, 1H), 5.35 (d, *J*=5 Hz, 1H), 5.16 (s, 2H), 4.46-4.52 (m, 1H), 3.71 (dd, half of ABX pattern, *J*=14.5, 6 Hz, 1H), 3.55 (dd, half of ABX pattern, *J*=14.5, 6 Hz, 1H), 1.43 (s, 3H), 1.42 (s, 3H).

ANCILLARY INFORMATION

Supporting Information. The experimental details for the preparation of final analogs **3, 17-46** are available free of charge via the Internet at http://pubs.acs.org.

PDB ID Codes. The PDB code for the cocrystal structure of compound **17** with *P. aeruginosa* PBP3 is 4L0L.

Corresponding author information. *Phone: (860) 441-3522. E-mail: matthew.f.brown@pfizer.com

Acknowledgement. We thank Jeffrey Van Deusen and Jennifer Winton for providing pharmacokinetic data. We thank Jim Bradow and Benjamin Hritzko for conducting analytical work critical to compound purification efforts. Finally, the authors would like to thank Mark Flanagan for helpful discussions and the manuscript reviewers and editors for providing useful feedback.

Abbreviations used. MIC, minimum inhibitory concentration; PBP, penicillin binding protein; MDR, multi-drug resistant; MHB, Mueller-Hinton broth.

REFERENCES

1. (a) Boucher Helen, W.; Talbot George, H.; Bradley John, S.; Edwards John, E.; Gilbert, D.; Rice Louis, B.; Scheld, M.; Spellberg, B.; Bartlett, J., Bad bugs, no drugs: no ESKAPE! An update from the Infectious Diseases Society of America. *Clin. Infect. Dis.* **2009,** *48*, 1-12; (b) Cooper, M. A.; Shlaes, D., Fix the antibiotics pipeline. *Nature (London, U. K.)* **2011,** *472*, 32.

2. (a) Wencewicz, T. A.; Moellmann, U.; Long, T. E.; Miller, M. J., Is drug release necessary for antimicrobial activity of siderophore-drug conjugates? Syntheses and biological studies of the naturally occurring salmycin "Trojan Horse" antibiotics and synthetic

desferridanoxamine-antibiotic conjugates. *BioMetals* **2009,** *22*, 633-648; (b) Ji, C.; Juarez-Hernandez, R. E.; Miller, M. J., Exploiting bacterial iron acquisition: siderophore conjugates. *Future Med. Chem.* **2012,** *4*, 297-313.

3. (a) Sykes, R. B.; Koster, W. H.; Bonner, D. P., The new monobactams: chemistry and biology. *J. Clin. Pharmacol.* **1988,** *28*, 113-119; (b) Barbachyn, M. R.; Tuominen, T. C., Synthesis and structure-activity relationships of monocarbams leading to U-78608. *J. Antibiot.* **1990,** *43*, 1199-203.

4. Flanagan, M. E.; Brickner, S. J.; Lall, M.; Casavant, J.; Deschenes, L.; Finegan, S. M.; George, D. M.; Granskog, K.; Hardink, J. R.; Huband, M. D.; Hoang, T.; Lamb, L.; Marra, A.; Mitton-Fry, M.; Mueller, J. P.; Mullins, L. M.; Noe, M. C.; O'Donnell, J. P.; Pattavina, D.; Penzien, J. B.; Schuff, B. P.; Sun, J.; Whipple, D. A.; Young, J.; Gootz, T. D., Preparation, Gram-negative antibacterial activity, and hydrolytic stability of novel siderophore-conjugated monocarbam diols. *ACS Med. Chem. Lett.* **2011,** *2*, 385-390.

5. (a) Page, M. G. P.; Dantier, C.; Desarbre, E., In vitro properties of BAL30072, a novel siderophore sulfactam with activity against multiresistant Gram-negative bacilli. *Antimicrob. Agents Chemother.* **2010,** *54*, 2291-2302; (b) Mushtaq, S.; Warner, M.; Livermore, D., Activity of the siderophore monobactam BAL30072 against multiresistant non-fermenters. *J. Antimicrob. Chemother.* **2010,** *65*, 266-270.

6. Arnould, J. C.; Boutron, P.; Pasquet, M. J., Synthesis and antibacterial activity of C-4 substituted monobactams. *Eur. J. Med. Chem.* **1992,** *27*, 131-140.

7. Mitton-Fry, M. J.; Arcari, J. T.; Brown, M. F.; Casavant, J. M.; Finegan, S. M.; Flanagan, M. E.; Gao, H.; George, D. M.; Gerstenberger, B. S.; Han, S.; Hardink, J. R.; Harris, T. M.; Hoang, T.; Huband, M. D.; Irvine, R.; Lall, M. S.; Megan Lemmon, M.; Li, C.; Lin, J.;

McCurdy, S. P.; Mueller, J. P.; Mullins, L.; Niosi, M.; Noe, M. C.; Pattavina, D.; Penzien, J.; Plummer, M. S.; Risley, H.; Schuff, B. P.; Shanmugasundaram, V.; Starr, J. T.; Sun, J.; Winton, J.; Young, J. A., Novel monobactams utilizing a siderophore uptake mechanism for the treatment of gram-negative infections. *Bioorg. Med. Chem. Lett.* **2012,** *22*, 5989-5994.

8. McPherson, C. J.; Aschenbrenner, L. M.; Lacey, B. M.; Fahnoe, K. C.; Lemmon, M. M.; Finegan, S. M.; Tadakamalla, B.; O'Donnell, J. P.; Mueller, J. P.; Tomaras, A. P., Clinically relevant gram-negative resistance mechanisms have no effect on the efficacy of MC-1, a novel siderophore-conjugated monocarbam. *Antimicrob. Agents Chemother.* **2012,** *56*, 6334-6342.

9. Kishimoto, S.; Sendai, M.; Tomimoto, M.; Hashiguchi, S.; Matsuo, T.; Ochiai, M., Chemical modification of sulfazecin. Synthesis of 4-methoxycarbonyl-2-azetidinone-1-sulfonic acid derivatives. *Chem. Pharm.Bull.* **1984,** *32*, 2646-2659.

10. Yamawaki, K.; Nomura, T.; Yasukata, T.; Uotani, K.; Miwa, H.; Takeda, K.; Nishitani, Y., A novel series of parenteral cephalosporins exhibiting potent activities against Pseudomonas aeruginosa and other Gram-negative pathogens: Synthesis and structure-activity relationships. *Bioorg. Med. Chem.* **2007,** *15*, 6716-6732.

11. Zhao, M. M.; Li, J.; Mano, E.; Song, Z. J.; Tschaen, D. M., Oxidation of primary alcohols to carboxylic acids with sodium chlorite catalyzed by tempo and bleach: 4-methoxyphenylacetic acid. *Org. Syn.* **2005,** *81*, 195-203.

12. (a) Bush, K.; Smith, S. A.; Ohringer, S.; Tanaka, S. K.; Bonner, D. P., Improved sensitivity in assays for binding of novel β-lactam antibiotics to penicillin-binding proteins of Escherichia coli. *Antimicrob. Agent Chemother.* **1987,** *31*, 1271-1273; (b) Georgopapadakou, N. H.; Smith, S. A.; Sykes, R. B., Mode of action of azthreonam. *Antimicrob. Agents Chemother.* **1982,** *21*, 950-956.

13. Han, S.; Zaniewski, R. P.; Marr, E. S.; Lacey, B. M.; Tomaras, A. P.; Evdokimov, A.; Miller, J. R.; Shanmugasundaram, V., Structural basis for effectiveness of siderophore-conjugated monocarbams against clinically relevant strains of Pseudomonas aeruginosa. *Proc. Natl. Acad. Sci. U. S. A.* **2010,** *107*, 22002-22007.

14. (a) Nikaido, H.; Rosenberg, E. Y., Cir and Fiu proteins in the outer membrane of Escherichia coli catalyze transport of monomeric catechols: study with β-lactam antibiotics containing catechol and analogous groups. *J. Bacteriol.* **1990,** *172*, 1361-1367; (b) Ghysels, B.; Ochsner, U.; Moellman, U.; Heinisch, L.; Vasil, M.; Cornelis, P.; Matthijs, S., The Pseudomonas aeruginosa pirA gene encodes a second receptor for ferrienterobactin and synthetic catecholate analogues. *FEMS Microbiol. Lett.* **2005,** *246*, 167-174.

15. (a) Crosa, J. H.; Walsh, C. T., Genetics and assembly line enzymology of siderophore biosynthesis in bacteria. *Microbiol. Mol. Biol. Rev.* **2002,** *66*, 223-249; (b) Poole, K.; McKay, G. A., Iron acquisition and its control in Pseudomonas aeruginosa: Many roads lead to Rome. *Front. Biosci.* **2003,** *8*, D661-D686; (c) Raymond, K. N.; Dertz, E. A.; Kim, S. S., Enterobactin: An archetype for microbial iron transport. *Proc. Natl. Acad. Sci. U. S. A.* **2003,** *100*, 3584-3588.

16. Gibson Ronald, L.; Burns Jane, L.; Ramsey Bonnie, W., Pathophysiology and management of pulmonary infections in cystic fibrosis. *Am. J. Respir. Crit. Care Med.* **2003,** *168*, 918-951.

17. Bush, K., Bench-to-bedside review: The role of beta-lactamases in antibiotic-resistant Gram-negative infections. *Crit. Care* **2010,** *14*, 224.

18. Carpenter, B. M.; Whitmire, J. M.; Merrell, D. S., This is not your mother's repressor: the complex role of Fur in pathogenesis. *Infect. Immun.* **2009,** *77*, 2590-2601.

19. CLSI. 2009a. Methods for dilution antimicrobial susceptibility tests for bacteria that grow aerobically: approved standard. Clinical Laboratory Standards Institute (CLSI). M07; CLSI. 2009b. Performance standards for antimicrobial susceptibility testing: 19th informational supplement. Clinical Laboratory Standards Institute(CLSI). M100.

20. Di, L.; Umland, J. P.; Trapa, P. E.; Maurer, T. S., Impact of recovery on fraction unbound using equilibrium dialysis. *J. Pharm. Sci.* **2012,** *101*, 1327-1335.

21. Zhao, G.; Meier, T. I.; Kahl, S. D.; Gee, K. R.; Blaszczak, L. C., BOCILLIN FL, a sensitive and commercially available reagent for detection of penicillin-binding proteins. *Antimicrob. Agents. Chemother.* **1999,** *43*, 1124-1128.

22. Corina, Molecular Networks: Erlangen, Germany

23. CVT, Pfizer: La Jolla, CA.

24. Omega, OpenEye Scientific Software: Santa Fe, NM.

25. ROCS, OpenEye Scientific Software: Santa Fe, NM.

26. MacroModel, version 9.0; Schrodinger, LLC: New York.

27. Kaminski, G. A.; Friesner, R. A.; Tirado-Rives, J.; Jorgensen, W. L., Evaluation and Reparametrization of the OPLS-AA Force Field for Proteins via Comparison with Accurate Quantum Chemical Calculations on Peptides. *J. Phys. Chem. B* **2001,** *105*, 6474-6487.

28. Takahashi, Y.; Yamashita, H.; Kobayashi, S.; Ohno, M., Synthetic study of cis-3-amino-4-(1-hydroxyalkyl)azetidin-2-ones using L-aspartic acid as a chiral synthon. *Chem. Pharm. Bull.* **1986,** *34*, 2732-2742.

Table of Contents graphic

for Table of contents only